Journal of Marine Science and Technology

Volume 29 | Issue 2 Article 13

Splitting The Scatter: Distinguishing Marine Organisms From Oceanographic Structures Using Acoustic Monitoring

Zhen Lu
Fisheries Resources Institute, Japan Fisheries Research and Education Agency,Japan, roshin@affrc.go.jp

Daisuke Hasegawa
Fisheries Resources Institute, Japan Fisheries Research and Education Agency,Japan

Takahiro Tanaka
Fisheries Resources Institute, Japan Fisheries Research and Education Agency,Japan

David M. Spencer
Fisheries Resources Institute, Japan Fisheries Research and Education Agency,Japan

Yuji Okazaki
Fisheries Resources Institute, Japan Fisheries Research and Education Agency,Japan

See next page for additional authors

Recommended Citation
Lu, Zhen; Hasegawa, Daisuke; Tanaka, Takahiro; Spencer, David M.; Okazaki, Yuji; and Okunishi, Takeshi (2021) "Splitting The Scatter: Distinguishing Marine Organisms From Oceanographic Structures Using Acoustic Monitoring," *Journal of Marine Science and Technology*: Vol. 29: Iss. 2, Article 13.
DOI: 10.51400/2709-6998.1083
Available at: https://jmstt.ntou.edu.tw/journal/vol29/iss2/13

Splitting The Scatter: Distinguishing Marine Organisms From Oceanographic Structures Using Acoustic Monitoring

Authors

Zhen Lu, Daisuke Hasegawa, Takahiro Tanaka, David M. Spencer, Yuji Okazaki, and Takeshi Okunishi

RESEARCH ARTICLE

Splitting the Scatter: Distinguishing Marine Organisms from Oceanographic Structures using Acoustic Monitoring

Zhen Lu*, Daisuke Hasegawa, Takahiro Tanaka, David M. Spencer, Yuji Okazaki, Takeshi Okunishi

Fisheries Resources Institute, Japan Fisheries Research and Education Agency, 3-27-5, Shinhama-cho, Shiogama-city, Miyagi, 985-0001, Japan

Abstract

In the northwest Pacific Ocean, off the Sanriku coast of Japan, convergence between the Tsugaru Warm Current (TWC) and the cold Oyashio Current (OC) results in the formation of highly dynamic oceanographic features that promote high biodiversity and generate hotspots for a range of commercially important fisheries. However, their effects on local biodiversity over much smaller spatiotemporal scales (<1 km) remains unclear. With the development of acoustic technology in recent years, echo-sounders are increasingly being used to conduct high-precision fishery resource assessments and detect small-scale variability in the oceanic thermohaline structure. In this study, we conducted a simultaneous hydrographic and dual-frequency echo-sounder survey to discriminate oceanographic features and marine organisms in the TWC-OC confluence zone. Echograms of acoustic backscatter measured at 38 kHz detected similar oceanographic features that were obtained from our hydrographic survey observations, but these features were less pronounced in the 120 kHz echograms. The dynamic oceanographic structure in the TWC-OC zone returned a large amount of backscatter, making it difficult to identify marine organisms from the scatter. The frequency differences of volume backscattering strength (*SV*) were, however, able to distinguish oceanographic structures from zooplankton detections. Outcomes from this study highlight the difficulty of distinguishing between hydrographic and biological detections in dynamic oceanographic environments. Further research into the acoustic frequency characteristics of heterogeneous hydrographic features will help better understand how species distributions are affected, so that the acoustic method can be used to provide more accurate estimates of species abundance.

Keywords: Acoustic backscattering, Oceanographic structure, Tsugaru warm and oyashio currents confluence zone, Undulating towed array

1. Introduction

Oceanographic environments enormously change over a broad range of spatial and temporal scales, and this fact dictates the presence, migration and survival of all marine species at different stages of their lifecycle [3]. The dynamic nature of the ocean generates areas of high and low productivity, which results sustained fishery hotspots and marine conservation zones. The convergence between the warm Tsugaru Warm Current (TWC) from the Sea of Japan and cold Oyashio Current (OC) from the subarctic northwest Pacific results in the formation of highly dynamic oceanographic mechanisms (e.g. eddies and fronts) off the Sanriku coast on the east side of northern Honshu, Japan (Shimizu et al., 2001) [9,13,22]. These mechanisms promote

Received 30 June 2020; revised 16 September 2020; accepted 18 September 2020.
Available online 21 May 2021.

* Corresponding author.
E-mail address: roshin@affrc.go.jp (Z. Lu).

https://doi.org/10.514/2709-6998.1083

high biodiversity and generate hotspots for krill, squid and many other commercially important fisheries [31,11]. While these areas are known hotspots for fisheries, there is limited information on whether species distributions change over small spatial scales (meters to kilometers) in accordance with fine-scale oceanographic structures that formed in these highly dynamic environments. The development of acoustic technology and its application in fishery resource assessments has the potential to elucidate some of these uncertainties.

Multi-frequency quantitative echosounders are increasingly being used for high-precision estimations of the distributions and abundances of organisms from small plankton to large demersal fish, with the advantages of short time, wide area and low-cost surveys [8,4]. The size and density of the organisms that make up the acoustic scattering layer can be estimated using the difference between the acoustic volume backscattering strengths (*SV*) of the high and low frequencies [6]. Besides direct echosounder observations, theoretical target strength (*TS*) models, such as the Distorted Wave Born Approximation (DWBA) model, can also be used to describe the differences in *SV* frequency characteristics [2,24]. Previous studies investigating predator and prey overlap were also able to discriminate a number of fish and plankton species using the frequency difference between *SV*s [18,26,10,12,30].

Sediments, air bubbles and gradients of temperature and salinity also contribute backscatter in the ocean, making it difficult to interpret the acoustic data [28,17]. Because of this sensitivity to physical structure in the water column, ship-mounted echo-sounders have been used to document variability in oceanic thermohaline structures and map the mixed layer depth (MLD) in the central Arctic Ocean [25]. However, the MLD was well-defined in this region and biological scattering did not dominate the acoustic return signal. In other regions, mixing processes often disturb temperature and salinity gradients, which can spread thermal and saline microstructures throughout the water column [7,27] and influence the acoustic signal. In areas with high biological activity and mixing, the MLD would be much harder to observe using a single-frequency echo-sounder, as these microstructures and plankton are often collocated and not easy to distinguish. Furthermore, oceanographic features can change frequently and rapidly, with the result that backscatter will show different characteristics at different times and in different areas. Although acoustic backscattering spectra from biological- and physical-scattering have different shapes that make it possible to differentiate and measure their scattering contributions [28,14,16], there has been limited research on distinguishing marine organisms and oceanographic structures in dynamic areas prone to substantial mixing.

In this study, we use the difference in *SV* from two frequencies to characterize the various levels of scatter. Combining the frequency characteristics and the data from a simultaneous hydrographic survey, we aimed to obtain accurate zooplankton distribution data by separating the mixed signals from oceanographic structures and marine organisms in the TWC-OC confluence zone.

2. Materials and Methods

2.1. Hydrographic survey

The survey was conducted along a transect crossing two frontal features in the TWC-OC confluence zone on July 26, 2019, aboard the *R/V Wakatakamaru* (Fig. 1). The survey transect was determined based on the daily (1 km resolution) sea surface temperature (SST) information, provided by the Japan Aerospace Exploration Agency (JAXA, www.eorc.jaxa.jp/ptree), and geostrophic current patterns derived from satellite altimeter (0.25° resolution) information, whichh was sourced from the Copernicus Marine Environment Monitoring Service (https://marine.copernicus.eu/).

Hydrographic observations were made using a high-resolution, undulating towed array (UTA, [23]). The array comprised three RINKO-Profilers (JAC, ASTD152), a real-time depth monitor (MARPORT, TD-7-00) and an underwater depressor (BE, V-Wing1220) at the end of the array. The multi-sensor profilers were used to collect both hydrographic (temperature, salinity, density) and biological data (chlorophyll, turbidity and dissolved oxygen) at a sampling rate of 10 Hz. Each component was attached to the cable of an onboard towing winch system (Tsurumi Seiki Ltd., 68HP hydraulic, WL: 3.5 ton, cable: φ10 mm × 8000 m) and undulations were carried out by winching the array up and down 150 m in the water column at a speed of about 0.6 m/s, while completing each undulation approximately every 8 min. Vertical profiles were collected for three sections of the water column while the ship travelled along the transect at speeds between 3 and 4.5 knots.

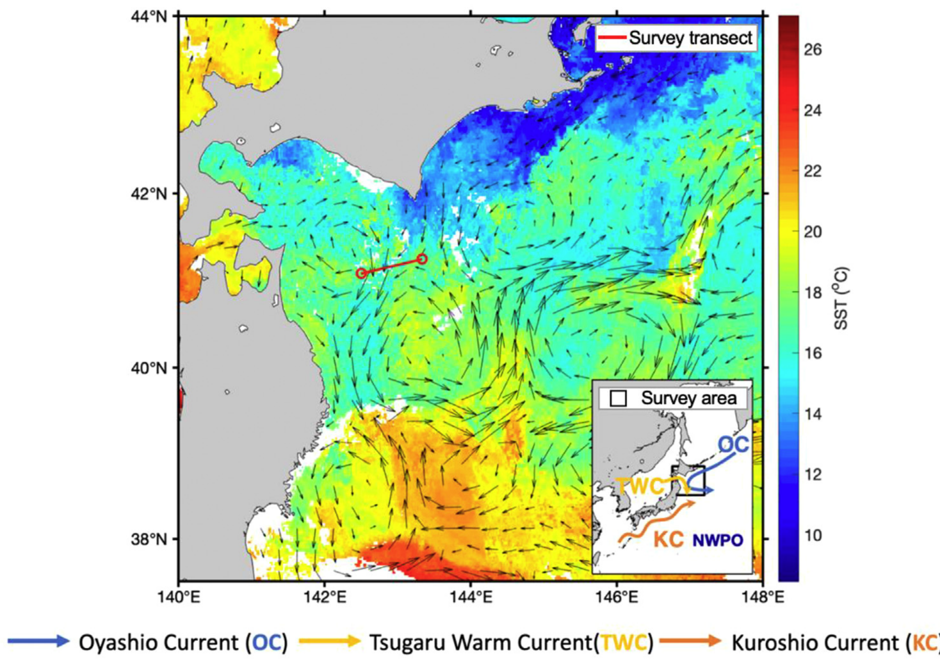

Fig. 1. Sea surface temperature (SST) and geostrophic current map of the TWC-OC confluence zone in the northwest Pacific Ocean (NWPO), off the Sanriku coast of Japan. Acoustic and hydrographic measurements were carried out across in the TWC-OC confluence zone (red 'Survey transect') on July 26, 2019. Surface features are illustrated for July 23, which was the closest day to July 26 when there was minimal cloud cover.

2.2. Acoustic measurement and data analysis

Acoustic measurements were conducted simultaneously with the UTA system. Acoustic backscatter was measured down to depths of 500 m using a quantitative echo-sounder KFC-3000 (Sonic) that operated at two frequencies, 38 kHz and 120 kHz, with a pulse width of 1.2 ms and pulse interval of 2 s. In order to get reliable results, in June, 2019, the KFC-3000 echosounder was calibrated pre-cruise using a tungsten-carbide sphere with the diameter of 38.1 mm (WC 38.1) following the method described by [5] for the transmitting and receiving system. The shipboard ADCP and other unnecessary acoustic equipment were turned off to prevent interference with the echo-sounder.

The raw acoustic data were post-processed using Echoview 10 (Australia, Echoview Software) by loading the pre-cruise calibration file and background noise was removed using the 'Background noise removal' function. Processed 'Sv value' data were then exported as mat files and the corresponding *SV* echograms were plotted and analyzed using MATLAB (Mathworks). The *SV* was averaged with the integration interval of 0.45 m × 10 ping as 1 cell.

2.3. Identification by frequency differences method

Marine organisms have inherent frequency characteristics based on body size and body composition, and so the relative frequency response is useful to differentiate different organisms on echograms [1].

When the scatter is widely distributed in an irregular pattern with respect to the beam opening, the volume backscattering strength (*SV*) is shown by the linear notation as:

$$SV = 10\log Sv = 10\log n + TS \tag{1}$$

$$TS = 10\log \sigma_{bs} \tag{2}$$

Here *Sv* is the volume backscattering coefficient and the linear value of *SV* (dB); n is the organism density (ind.m^{-3}) of fish; *TS* (dB) is the target strength; and σ_{bs} is the acoustic backscattering cross-section, the linear value of *TS*. In Eq. (1), n is constant when the same range is detected at multiple frequencies so that the frequency characteristics of *SV* is equal to the frequency characteristics of *TS*. *TS* characterizes the intensity of the acoustic backscattering signal and is a quantitative measure of the size of marine organisms.

The difference between the SVs of the two frequencies is represented using ΔSV. The following equation can be obtained from the differences of Eq. (1) using different frequencies.

$$\Delta SV_{H-L} = SV_H - SV_L \tag{3}$$

whereby the difference between the frequencies 38 kHz and 120 kHz are denoted as ΔSV_{120-38}. These last values will be used to delineate acoustic backscattering from oceanographic structure and zooplankton in this study.

3. Results and Discussion

3.1. Observation results from UTA and KFC3000

Combining the UTA system and quantitative echo-sounder, we were able to simultaneously measure the oceanographic structures and biological distributions in the TWC-OC confluence zone. The UTA trial took place between 11:30 and 17:00 (UTC +9 hrs), 40 undulations over a distance of 38 km were carried out to collect a total of 240 vertical profiles and covered. The vertical cross-sectional distribution of water temperature and salinity obtained by UTA captured fine horizontal and vertical structure in the upper 150 m, with a horizontal resolution (distance travelled for each undulation) of 450 m (Fig. 2). Low-temperature and low-salinity OC water made up the most part of the water column east of 143 °E, which was then subducted beneath the TWC westward along the whole survey transect. A small-scale OC water mass was also found at depths of about 30-50 m near 142.9 °E. High-temperature and high-salinity TWC water were more pronounced at the western part of the transect. High-temperature and low-salinity surface water in the top 15 m of the water column was distributed along the whole survey transect. The cross-mixing of TWC-OC waters formed clear thermal and saline structures (Fig. 2). The density of the water gradually increased from the upper layer to the lower layer, and the change was sharp within the depth of 50m where the OC water changed more drastically than the TWC water did.

The echo shape of the 38 kHz *SV* echogram corresponded with the salinity characteristics measured by UTA (Fig. 3). Similar echoes were also observed in the 120 kHz data, but features were less pronounced. In other words, where the salinity changed greatly, an echo signal response appeared, and the signal was stronger at the low frequency. In addition, the form and distribution of echoes was clearly different between the upper and lower sections of 30 m, in a way similar to salinity contours which implies that the type or density of the scatter sources may be different. Towards the east patch signals were stronger at 120 kHz at around 60 to 100 m, but no obvious changes in the salinity structure were observed there. The ΔSV method has been proved to be one of the effective methods to solve this problem.

3.2. Distinguishing oceanographic structure and zooplankton

The calculated ΔSV_{120-38} was classified into three groups: (a) 1 to 25 dB, (b) −5 to 1 dB, (c) −25 to −5 dB (Fig. 4) based on the frequency characteristics of different scatters as described in previous studies Namely, group (a) has been found to represent zooplankton, small bladderless fish and suspended sediment; group (b) represented large fish with a swim-bladder and bladderless fish; and group (c) represents both small fish with swim-bladders and physical oceanographic microstructures [18,26,10,28,14,15,20,12,30].

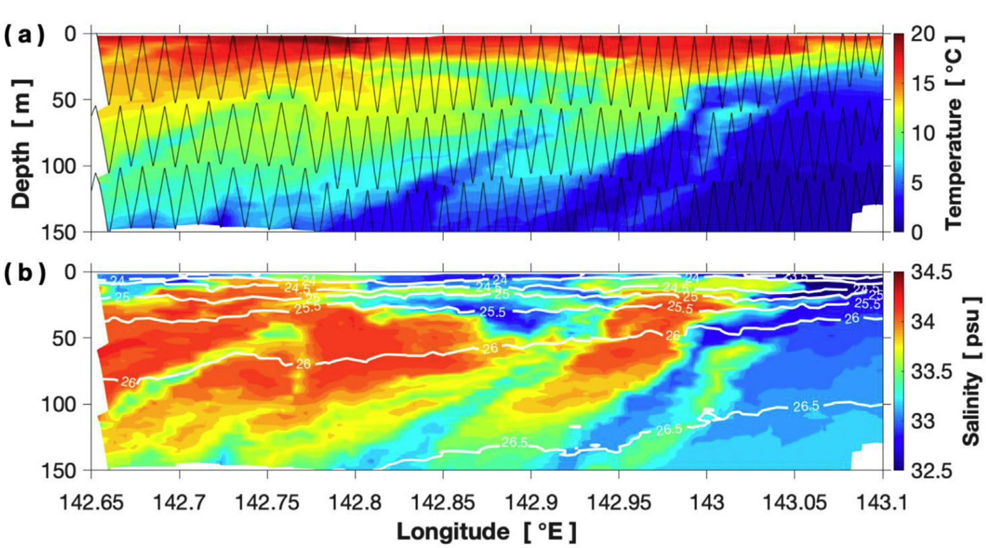

Fig. 2. Contour plots of temperature (a), salinity (b) from UTA. Black lines on (a) illustrated the undulation profiles of the three RINKO sensors and white lines on (b) were the water density contour lines.

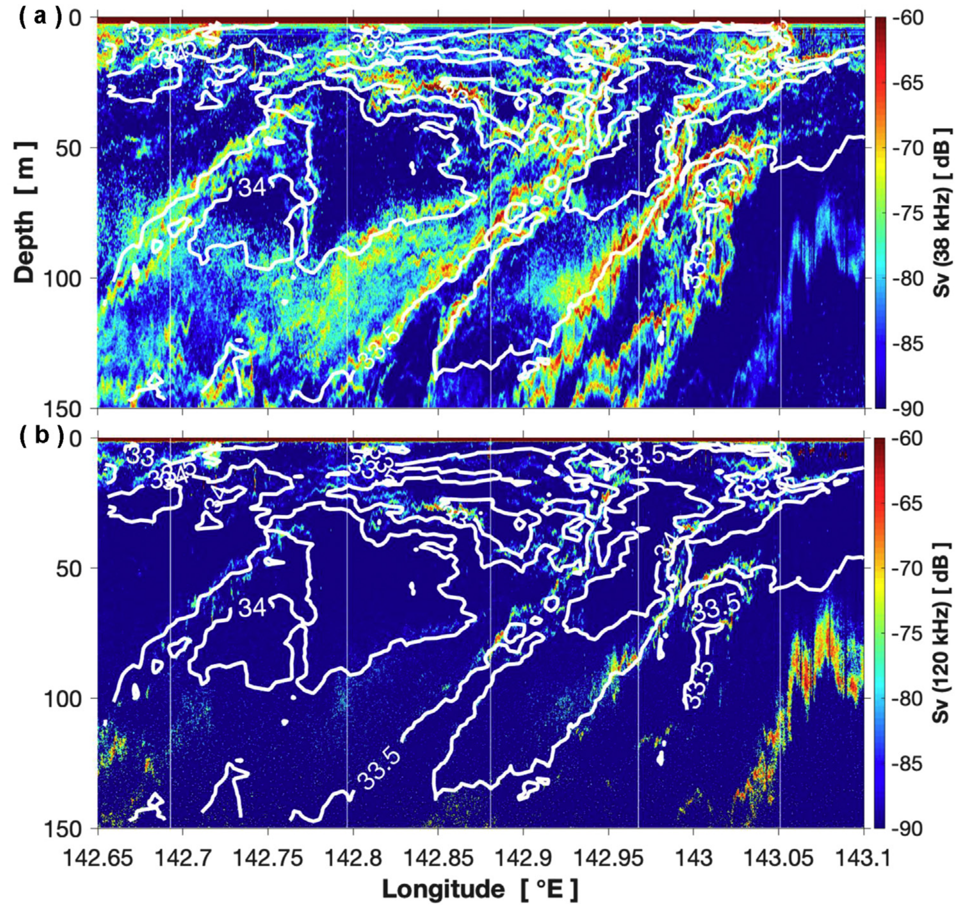

Fig. 3. Echograms of acoustic volume backscattering strength, SV, recorded by KFC-3000 at the frequencies of 38 kHz (a) and 120 kHz (b). In order to observe the echo signals more clearly, the color bar had been adjusted. White lines on the echograms are the salinity contour lines from 32.5 to 34.5 psu at the interval of 0.5 psu.

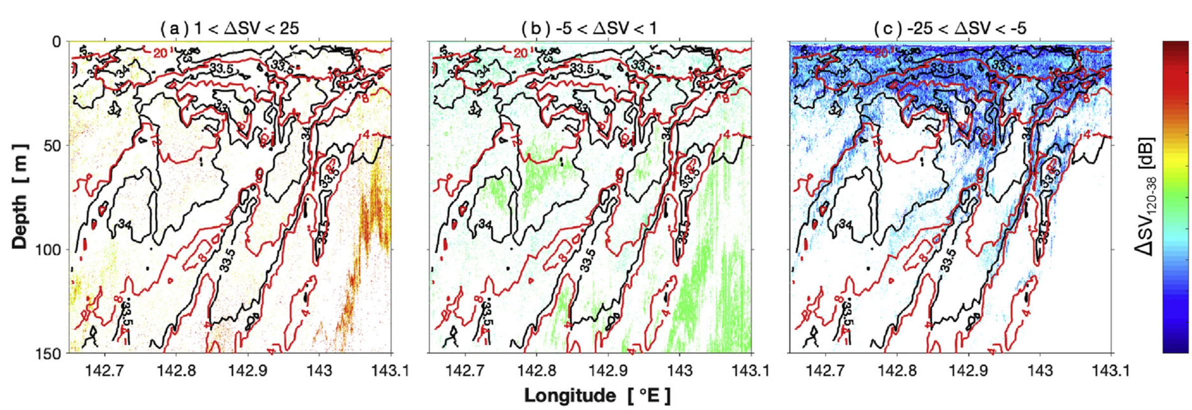

Fig. 4. Echograms of calculated $\Delta SV_{120\text{-}38}$ which were classified to three groups of (a) 1 to 25 dB, (b) −5 to 1 dB, (c) −25 to −5 dB, respectively. Black lines on the echograms illustrate the salinity contour lines from 32.5 to 34.5 psu at the interval of 0.5 psu and red lines are the water temperature contour lines from 0 to 20 °C at the interval of 4 °C.

The three groups showed different echo distribution. In the upper 30 m, all three groups showed complex echoes without obvious frequency characteristics, which could not be separated effectively (Fig. 4). A stronger patch signal was seen around 100 m depths on the Oyashio side (right) where the water temperature was lower than 4 °C in group (a), whereas it could not be seen in groups (b) and (c)

(Fig. 4). In addition, this signal had lager value of ΔSV_{120-38} than other signals in group (a). From a few NORPAC net samples (0~150 m) collected during the same cruise, we found that the Oyashio side (41.20 °N, 143.08 °E) had a higher proportion of copepod, while the proportion of krill was higher in the west (41.18 °N, 143.00 °E) (data is not shown in this paper). These anomalous detections on the Oyashio side in group (a) were therefore likely to be dominated by copepods, and other. Weaker signals may be mainly scattered from krill. These results agree with those of a previous study [19] that reported krill fishing grounds formed in the mixed area of 7-9 °C (Fig. 4a). On the other hand, the results also consistent with characteristic acoustic property that ΔSV_{120-38} of copepod is higher than that of krill [12].

In the waters below 30 m, the echo became distributed along the contours of water temperature and salinity in ΔSV_{120-38} group (c) (Fig. 4c). Similar shaped echo shapes were also observed in ΔSV_{120-38} groups (a) (Fig. 4a), but they were very weak. The ΔSV_{120-38} of group (b) below the depth of 30 m was mostly 0 dB and its distribution appears to fill the space surrounding the backscatter observed in groups (a) and (c) (Fig. 4). Although these two groups exhibited similar patterns, prior research [28,14] suggests group (c) should correspond to oceanographic structures and that the other sorts of analysis described below are needed to differentiate between the two groups.

The different ΔSV groups were compared to vertical changes in salinity and temperature. Second-order gradients of 5 m vertically averaged temperature and salinity data were plotted against the 38 kHz SV (SV_{38}) for each ΔSV_{120-38} group (Fig. 5). It can be clearly seen that the second-order gradients in temperature changed proportionally with those in salinity. Occasionally SV_{38} was very large when the change in vertical gradients were small; but in general, SV_{38} was also very large when the change in the vertical gradients of temperature and salinity were large (Fig. 5-ALL). Specific to each ΔSV_{120-38} group, SV_{38} tended to increase as the change in the vertical gradient of water temperature and salinity increased in group (c), but SV_{38} did not increase for groups (a) and (b). Referring to [14]; when changes in temperature and salinity are proportional, ΔSV_{120-38} is about -10 dB from the upper bound model [29,21]. In general, the contour of temperature and salinity was similar (Fig. 4). These results further support the conclusion that the acoustic scattering from the lowest ΔSV_{120-38} range (group (c)) represent structure along the survey transect.

In this study, we classified ΔSV_{120-38} into three groups of echoes and were able to prove the existence of scatters caused by the oceanographic structures (as observed with UTA) by analyzing the relationship between SV_{38} and changes in vertical gradient of salinity and temperature. The groups (a) and (c) obtained by splitting the echo were both weakened compared to the original due to the overlap of zooplankton and oceanographic structure. The "noise" from oceanographic structure ultimately prevented accurate estimations of zooplankton abundance in the survey region. Therefore, as an important issue in the future, it will be necessary to study the acoustic characteristics of different hydrographic structures produced by the mixing of currents with different ranges of temperatures and salinity. Accounting more precisely for influence of the oceanographic structure will enable high precision quantitative fishery resource assessments in dynamic marine environments. High-speed development of broadband acoustic technology has the potential to resolve these issues, but

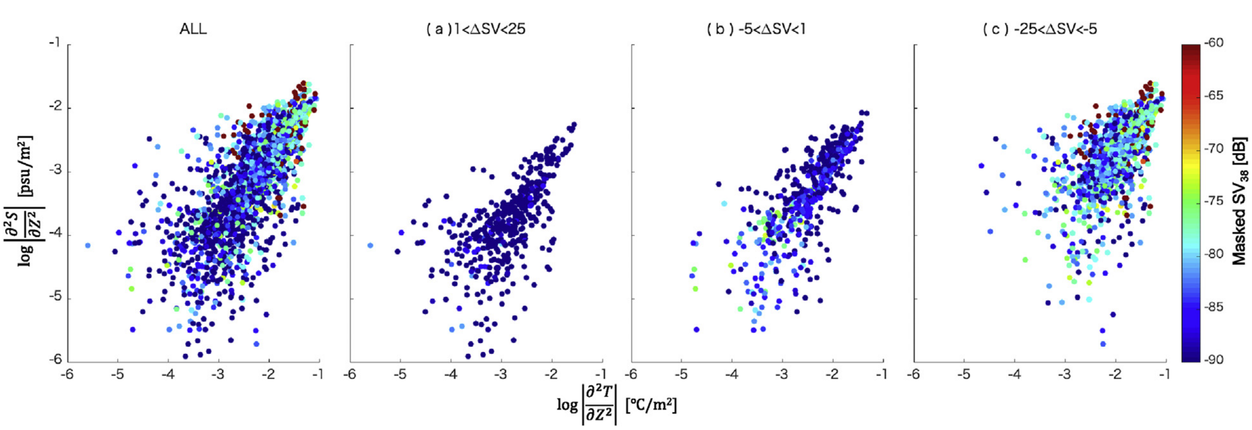

Fig. 5. Relationship between SV_{38} and changes in vertical gradient of salinity and temperature for all data and three $\Delta SV_{120\text{-}38}$ groups of (a) 1 to 25 dB, (b) −5 to 1 dB, (c) −25 to −5 dB.

requires careful interpretation of *SV* and the various sources of backscatter (e.g. biological and hydrographic).

4. Conclusion

There have been many reports to use the frequency differences of *SV* to distinguish biological species to better understand predator-prey overlap (e.g. walleye pollock and krill or pointhead flounder and juvenile walleye pollock), and predator competition (e.g. krill and copepod). However, few studies have had the aim of discriminating between biological and physical structures, especially in dynamic environments in which the hydrological conditions and biological composition are complex. To address this knowledge gap, we conducted simultaneous hydrographic and fishery resource surveys using a high-resolution oceanographic observation system (UTA) and a dual-frequency quantitative echo-sounder (KFC-3000) in the TWC-OC confluence zone. The UTA time series data for temperature and salinity resolved fine-scale spatial variability of different water mass systems along the survey transect. The results from the acoustic monitoring showed that the oceanographic structure returned a vast amount of backscatter, which prevented accurate estimates of marine organism populations. However, oceanographic structures and zooplankton could be distinguished using the difference between 38 kHz and 120 kHz volume backscattering strengths. These preliminary findings highlight the complex nature of backscatter in such highly dynamic oceanic environments, making it difficult to achieve high precision quantitative fishery resource assessments using the conventional methods. The use of high-speed development of broadband acoustic technology to separate the physical oceanographic structure from marine organisms has potential and merits further investigation.

Acknowledgements

The authors thank the captain and crew of the *R/V Wakataka Maru* for their kind assistance during the surveys. We gratefully acknowledge Ph.D. Imaizumi and other members of fisheries information science group of National Research Institute of Fisheries Engineering for helping calibrate the echo-sounder and providing constructive comments. This work was supported by the research grant (No. JPMJCR19F1) of core research for evolutionary science and technology from Japan Science and Technology Agency. This paper was improved following comments from anonymous reviewers and editors.

References

[1] Benoit-Bird KJ, Lawson GL. Ecological Insights from Pelagic Habitats Acquired Using Active Acoustic Techniques. Annu Rev Mar Sci 2016;8:463–90.

[2] Chu D, Foote KG, Stanton TK. Further analysis of target strength measurements of Antarctic krill at 38 and 120 kHz: Comparison with deformed cylinder model and inference of orientation distribution. J Acoust Soc Am 1993;93:2985–8.

[3] Drinkwater KF, Beaugrand G, Kaeriyama M, Kim S, Ottersen G, Perry RI, et al. On the processes linking climate to ecosystem changes. J Mar SysT 2010;79:374–88.

[4] Fernandes PG, Gerlotto F, Holliday DV, Nakken O, Simmonds EJ. Acoustic applications in fisheries sciences: the ICES contribution. ICES Mar Sci Symp 2002;215:483–92.

[5] Foote KG, Knudsen HP, Vestnes G, MacLennan DN, Simmonds EJ. Calibration of acoustic instruments for fish density estimation: a practical guide. Technical Report ICES Cooper Res Rep 1987;144.

[6] Furusawa M. Study on echo sounding for estimating fisheries resources. Bull Nat Res Inst Fish Eng 1990;11:173–249 (in Japanese, with English Abstract).

[7] Gregg M. Diapycnal mixing in the thermocline: a review. J Geophys Res 1987;92:5249–86.

[8] Iida K, Mukai T, Hwang D. Relationship between acoustic backscattering strength and density of zooplankton in the sound-scattering layer. ICES J Mar Sci 1996;53:507–12.

[9] Isoda Y, Suzuki K. Interannual variations of the Tsugaru gyre551. Hokkaido University: Bulletin of Fisheries Sciences; 2004. p. 71–4 (in Japanese, with English Abstract).

[10] Kang M, Furusawa M, Miyashita K. Effective and accurate use of difference in mean volume backscattering strength to identify fish and plankton. ICES J Mar Sci 2002;59:794–804.

[11] Kawabata A. Distribution pattern of Japanese common squid, *Todarodes pacificus*, related to its habitat in waters off northern Sanriku coast of Japan. Rep Annu Meet Squid Res 2004;32:8–12 (in Japanese).

[12] Kim U, Mukai T, Iida K. Acoustic identification of krill and copepods using frequency differences of volume backscattering strength around Funka Bay, Hokkaido, Japan. Nippon Suisan Gakkaishi 2016;82:587–600 (in Japanese, with English Abstract).

[13] Kobayashi N, Isoda Y, Asahi K. Numerical experiment for a westward tail of the Tsugaru Gyre along the Hidaka shelf slope. Oceanogr Jpn 2015;24:171–87 (in Japanese, with English Abstract).

[14] Lavery AC, Schmitt RW, Stanton TK. High-frequency acoustic scattering from turbulent oceanic microstructure: The importance of density fluctuations. The Journal of the Acoustical Society of America 2003;114:2685–97.

[15] Lavery AC, Wiebe PH, Stanton TK, Lawson GL, Benfield MC, Copley NC. Determining dominant scatterers of sound in mixed zooplankton populations. J Acoust Soc Am 2007;122:3304–26.

[16] Lavery AC, Chu D, Moum JN. Observations of broadband acoustic backscattering from nonlinear internal waves: assessing the contribution from microstructure. IEEE J Ocean Eng 2010;35:695–709.

[17] Lu Z, Hasegawa D, Takahiro T, Spencer DM, Okazaki Y, Okunishi T. Distinguishing acoustic backscattering from oceanographic structure and zooplankton. In: The program and abstracts of the Japanese society of fisheries science spring meeting 2020; 2020. p. 4 (in Japanese).

[18] Miyashita K, Aoki I, Seno K, Taki K, Ogishima T. Acoustic identification of isada krill, *Euphausia pacifica* Hansen, off the Sanriku coast, north-eastern Japan. Fish Oceanogr 1997;6: 266–71.

[19] Odate K. An euphausid crustacea exploited along the sanriku and joban coast. Bull Tohoku Reg Fish Res Lab 1979;40: 15–25 (in Japanese, with English Abstract).

[20] Robertis AD, McKelvey DR, Resslera PH. Development and application of an empirical multifrequency method for

backscatter classification. Can J Fish Aquat Sci 2010;67: 1459–74.
[21] Seim HE. Acoustic backscatter from salinity microstructure. J Atmos Ocean Technol 1999;16:1491–8.
[22] Shimizu Y, Yasuda I, Ito S. Distribution and Circulation of the Coastal Oyashio Intrusion. J Phys Oceanogr 2001;31: 1561–78.
[23] Spencer DM, Hasegawa D, Takahiro T, Lu Z, Okazaki Y, Okunishi T. An Undulating Towed Array (UTA) for high-resolution observations of the upper ocean. 2020. Ocean Sciences Meeting 2020, San Diego, USA.
[24] Stanton TK, Chu D. Review and recommendations for the modelling of acoustic scattering by fluid-like elongated zooplankton: euphausiids and copepods. ICES J Mar Sci 2000;57:793–807.
[25] Stranne C, Mayer L, Jakobsson M, Weidner E, Jerram K, Weber TC, et al. Acoustic mapping of mixed layer depth. Ocean Sci Discuss 2018;14:503–14.
[26] Swartzman G, Brodeur R, Napp J, Hunt G, Deme D, Hewitt R. Spatial proximity of age-0 walleye pollock (Theragra chalcogramma) to zooplankton near the Pribilof Islands, Bering Sea, Alaska. ICES J Mar Sci 1999;56:545–60.
[27] Thorpe SA. Transitional phenomena and the development of turbulence in stratified fluids: a review. J Geophys Res 1987; 92:5231–48.
[28] Warren JD, Stanton TK, Wiebe PH, Seim HE. Inference of biological and physical parameters in an internal wave using multiple-frequency, acoustic-scattering data. ICES J Mar Sci 2003;60:1033–46.
[29] Washburn L, Duda TF, Jacobs DC. Interpreting conductivity microstructure: Estimating the temperature variance dissipation rate. J Atmos Ocean Technol 1996;13:1166–88.
[30] Yan N, Mukai T, Yamamoto J, Hasegawa K. Acoustic discrimination between juvenile walleye pollock and point-head flounder. Fish Res 2020;224:105434.
[31] Yasuda I, Okuda K, Hirai M, Ogawa Y, Kudoh H, Fukushima S, et al. Short-term variations of the Tsugaru Warm Current in autumn. Bull Tohoku Reg Fish Res Lab 1988;50:153–91.